Burnout of the Organic Vehicle in an Electrically Conductive Thick-Film Paste

ZONGRONG LIU[1] and D.D.L. CHUNG[1,2]

1.—Composite Materials Research Laboratory, University at Buffalo, State University of New York, Buffalo, NY 14260. 2.—E-mail: ddlchung@buffalo.edu

The burnout of the organic vehicle in a silver-particle, glass-free, electrically conductive, thick-film paste during firing in air was studied. For a vehicle consisting of ethyl cellulose dissolved in ether, burnout primarily involves the thermal decomposition of ethyl cellulose. The presence of ether with dissolved ethyl cellulose facilitates the burnout of ethyl cellulose. Excessive ethyl cellulose hinders the burnout. A high heating rate results in more residue after burnout. By interrupting the heating at 160°C for 15 min, the residue after subsequent burnout is diminished probably because of reduced temporal overlap of the processes of organic burnout and silver particle necking. By interrupting the heating at either 300°C or 385°C for 30 min, the temperature required for complete burnout is reduced. The addition of silver particles facilitates drying at room temperature and burnout upon heating.

Key words: Thick-film paste, electrically conductive, organic vehicle, burnout, thermal analysis, calorimetry

INTRODUCTION

Organic additives are widely used in ceramic slurry preparation (as in tape casting and gelcasting[1–8]), green compact fabrication (as in powder metallurgy[9–19]), thick-film materials development,[20–24] and other applications.[25–29] The ingredients are typically functional phases in the form of solids, and organic additives in the form of liquids, solutions, or suspensions. The ingredients are mixed to form a paste. The purpose of the addition of organic ingredients is to facilitate the fabrication of functional materials with appropriate combinations of shape, density, and strength before firing. The organic additives are removed, usually in the early part of the firing process.

Because complete removal of organic components prior to densification is critical to obtaining defect-free products, numerous investigations,[1–3,11,15,16,30] both experimental and theoretical, have been conducted on the removal of organic components in tape casting, gelcasting, and powder metallurgy. The removal of organic components is generally called organic burnout or pyrolysis. This process involves evaporation and thermal and/or oxidative degradation[1,2,31–35] of the organic components. The organic burnout usually involves[2,11] the removal of volatile components, namely, molecules with low molecular weight at relatively low temperatures, followed by the removal of the nonvolatile components at higher temperatures. In air, the organic additives can be decomposed and oxidized to form CO_2, CO, water, and other small organic molecules.[33] Incomplete organic burnout usually results in poor performance, such as low density, poor mechanical strength, and poor electrical, thermal, or thermoelectric properties, for the final product.[35,36]

Electrically conductive, thick-film pastes are widely used for electrical interconnections in electronic packaging. Although there are numerous studies on the organic burnout in tape casting or powder metallurgy, few investigations about the organic burnout in thick-film materials have been performed. Unlike the relatively large size of the green parts in tape casting or powder metallurgy, the largest thickness of thick films is usually less than 100 μm (as for the cathode in a solid-oxide fuel cell), and most other functional thick films have a thickness less than 30 μm. Because of the difference in size, different organic-burnout mechanisms may

(Received March 18, 2004; accepted June 18, 2004)

occur in thick-film pastes compared to pastes in tape casting or powder metallurgy. Therefore, this paper is focused on studying the process of organic burnout in electrically conductive, thick-film pastes.

Organic burnout is commonly assumed to occur at temperatures far below the temperature at which sintering takes place in tape casting or powder metallurgy. No information on the possible temporal overlap of the processes of burnout and sintering has been reported. However, the two processes may overlap, particularly in the case of low-temperature fireable compositions, which are of current interest to the electronic industry because of the associated processing cost reduction. It is possible for the two processes to affect one another. In particular, the overlap of the two processes may hinder the burnout of the organic components. Understanding the burnout of organic components in thick-film materials is valuable for the formation of thick-film pastes and for the development of the firing procedure.

In this work, in order to understand the science of the organic-burnout process, the effects of the various ingredients on the burnout process were systematically investigated. The ingredients were silver particles, solvent, and solute, as chosen to keep the formulation simple for the purpose of studying the organic-burnout process. Glass frit was absent, as it is not needed for glass-free pastes, which use minor metal ingredients, such as titanium, to provide bonding.[22] The effects of heating rate and interrupted heating on the burnout were also studied.

Thermal analysis was used in this work to monitor the burnout process in real time. Microscopy was used to examine the microstructure of the thick film after firing at various temperatures that are relevant to the burnout process. The thermal analysis encompassed monitoring both the enthalpy change and the weight in the early stage of firing. The enthalpy change monitoring involved differential scanning calorimetry (DSC), conducted up to 500°C. The weight monitoring involved thermogravimetric analysis (TGA) up to 900°C.

This work also includes a brief study of the process of drying in air at room temperature, as drying is a process that is commonly conducted in the industry prior to burnout, and the effects of the various ingredients on the drying process are possibly related to the effects of the ingredients on the burnout process.

EXPERIMENTAL METHODS

To simplify the formulation for facilitating organic-burnout result interpretation, silver powder rather than silver alloy powder was used to develop a glass-free, thick-film composition, even though silver alloy (e.g., Ag-Cu alloy) powder is used in glass-free pastes.[22] The organic vehicle consisted of 40 wt.% ethyl cellulose and 60 wt.% di(ethylene glycol) butyl ether. The ratio of silver powder to the organic vehicle in the paste was 3:1 by weight. The silver particles, which were irregularly shaped, had a size ranging from 1.5 μm to 2.5 μm. The standard, commercial alumina substrate (96% Al_2O_3, 50.8 mm × 50.8 mm × 0.6 mm) was used.

Ethyl cellulose (98%) was supplied by Dow Chemical Company (Midland, MI). Di(ethylene glycol) butyl ether (>99%) (referred to as ether in this paper) was purchased from Aldrich Chemical Company, Inc. (Milwaukee, WI). The silver powder was purchased from AMES Goldsmith Corp. (Glens Falls, NY).

In the scanning electron microscopy (SEM) part of this work, the silver particle pastes were applied on substrates, which were alumina. The paste was applied manually. The firing was conducted in air at 300°C, 350°C, or 385°C for 30 min, all with a heating rate of 15°C/min and a cooling rate of 40°C/min. All the samples were fired after drying in air at room temperature for 2 days. The surface morphology of the thick films after air firing at various temperatures was examined by SEM. Microscopy was not performed on formulations without silver although thermal analysis was performed on formulations with and without silver.

To analyze the effects of different components in the thick-film composition on the organic burnout of the thick film, DSC and TGA were conducted for (1) ethyl cellulose by itself, (2) ether by itself, (3) solutions of 40 wt.% or 70 wt.% ethyl cellulose in ether, and (4) thick-film paste (i.e., silver powder suspended in the organic vehicle mentioned previously, without a substrate). The materials were put in aluminum DSC pans and covered by aluminum lids for DSC testing, which was conducted in air using a Perkin-Elmer Corp. (Norwalk, CT) DSC 7 system. The specimens were heated up to 500°C at a heating rate of either 7°C/min or 15°C/min. A Perkin-Elmer TGA 7 system was used for the TGA, which was conducted upon heating to either 700°C or 900°C at a heating rate of 7°C/min, 15°C/min, or 50°C/min.

The drying process was studied briefly by visual/manual observation in order to determine the time taken for drying to take place. The effects of the various components on the time needed for drying were thus investigated.

RESULTS AND DISCUSSION

Burnout Process Monitored by TGA

Figure 1 shows the typical, TGA weight-loss curves of (a) ether, (b) ethyl cellulose, (c) a solution of 40 wt.% ethyl cellulose in ether, and (d) thick-film paste, all at a heating rate of 15°C/min. As shown in curve a, about 99.5 wt.% of the ether evaporated below 185°C and its complete evaporation occurred below 300°C. As shown in curve b, about 80 wt.% of ethyl cellulose was burnt out below 320°C and about 97.5 wt.% was burnt out below 475°C. As shown in curve c, about 93.4 wt.% of the solution of 40 wt.% ethyl cellulose was burnt out below 320°C and about 99.4 wt.% of the solution was burnt out below 485°C. As shown by

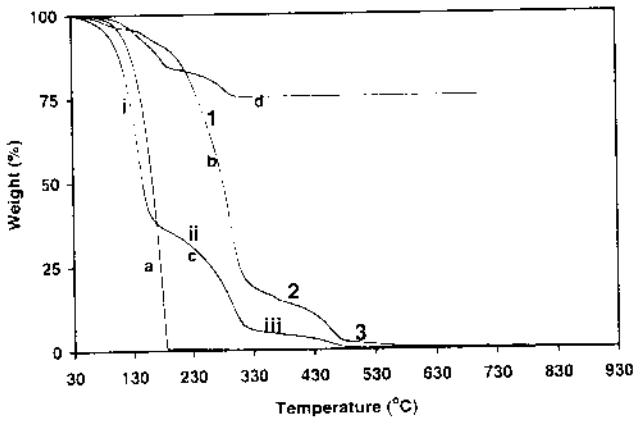

Fig. 1. The TGA curves of (a) ether, (b) ethyl cellulose, (c) a solution of 40 wt.% ethyl cellulose in ether, and (d) thick-film composition. The heating rate is 15°C/min.

comparison of curves b and c, the addition of ether to ethyl cellulose facilitated the organic burnout.

Curve d shows that the organic vehicle in the thick-film paste was completely burnt out below 320°C, implying that the addition of silver particles further helps the organic burnout. This means that the addition of metal particles helps the thermal decomposition of ethyl cellulose probably because of the high thermal conductivity of the metal particles and the separation of the organic molecules by the dispersed metal particles. Because of the high thermal conductivity, the thermal decomposition of the organic components may occur at the outside and inside parts of a thick-film paste almost at the same time. Hence, in the presence of the metal, complete removal of ethyl cellulose occurs at a relatively lower temperature. Without the metal particles, the thermal decomposition probably occurs from the outside to the inside because of the higher temperature at the surface.

Table I shows the remaining weight of (a) ethyl cellulose, (b) a solution of 40 wt.% ethyl cellulose in ether, and (c) thick-film paste during heating to selected temperatures during TGA testing. Table I (A and B in comparison) indicates that the addition of the ether to ethyl cellulose helps the organic burnout, so that complete burnout is achieved at lower temperatures. This is probably due to the higher tendency for separation and disentanglement of the ethyl cellulose molecules in the presence of ether. Table I (B and C in comparison) also shows that the addition of silver powder to the organic vehicle helps the organic burnout.

Figure 2 shows the typical TGA curves of weight and derivative weight (i.e., derivative of weight relative to temperature) versus temperature of (a) ether, (b) ethyl cellulose, (c) a solution of 40 wt.% ethyl cellulose in ether, and (d) thick-film paste. All TGA curves were obtained at a heating rate of 15°C/min. Evaporation of ether itself occurs upon heating above 30°C (Fig. 2a). However, evaporation of the majority of ether occurs above 110°C. Most ether evaporates below 185°C. The derivative weight-loss curve of the ethyl cellulose itself (Fig. 2b) has two peaks, in contrast to the single peak for ether (Fig. 2a). This is consistent with the multiple stages of weight loss shown by the curve of weight versus temperature in Fig. 2b.

Simultaneous TGA and differential thermal analysis (DTA) of a polymethyl methacrylate (PMMA) solution in Ref. 2 showed that an exothermic DTA peak is associated with a peak in the derivative TGA curve. Two exothermic DTA peaks were observed. The lower temperature peak was identified as being caused by the removal of low molecular-weight components, whereas the higher temperature peak was identified as being caused by the removal of nonvolatile components.[2]

For ethyl cellulose by itself (Fig. 2b), the main derivative TGA peak in the range from 185°C to 350°C is attributed to the thermal decomposition of ethyl cellulose. Simultaneous TGA and DTA testing of PMMA in Ref. 34 suggested that the removal of high molecular-weight components involved thermal decomposition at low temperatures and oxidative degradation at high temperatures. In Fig. 2b, the small derivative TGA peak from 395°C to 495°C may thus be due to oxidative degradation of the remaining ethyl cellulose. A third stage of weight loss occurs above 460°C, as shown by the curve of weight versus temperature (Fig. 2b). However, a corresponding derivative TGA peak is absent (Fig. 2b), possibly because of the small amount of residue; the oxidation of which presumably results in the weight loss in the third stage.

For the solution of 40 wt.% ethyl cellulose in ether, three peaks at 30–190°C, 190–340°C, and 340–495°C are shown in the derivative TGA curve (Fig. 2c), indicating three steps in the burnout. This

Table I. The Remaining Weight (%) during Heating of A (Ethyl Cellulose), B (Solution of 40 wt.% Ethyl Cellulose in Ether), and C (Thick-Film Paste) at Various Temperatures during TGA Testing at a Heating Rate of 15°C/min

	Temperature (°C)											
Composition	**250**	**300**	**350**	**400**	**450**	**480**	**500**	**550**	**600**	**650**	**700**	**750**
A	70.06	29.86	16.77	12.89	6.71	2.34	1.94	1.07	0.65	0.58	0.53	0.47
B	27.51	12.11	5.25	4.07	2.22	0.74	0.59	0.48	0.44	0.43	0.42	0.38
C	6.34*	0.77*	0.47*	0.47*	0.47*	0.47*	0.47*	0.47*	0.46*	0.44*	0.44*	—

*Remaining weight of the vehicle portion of the thick-film paste.

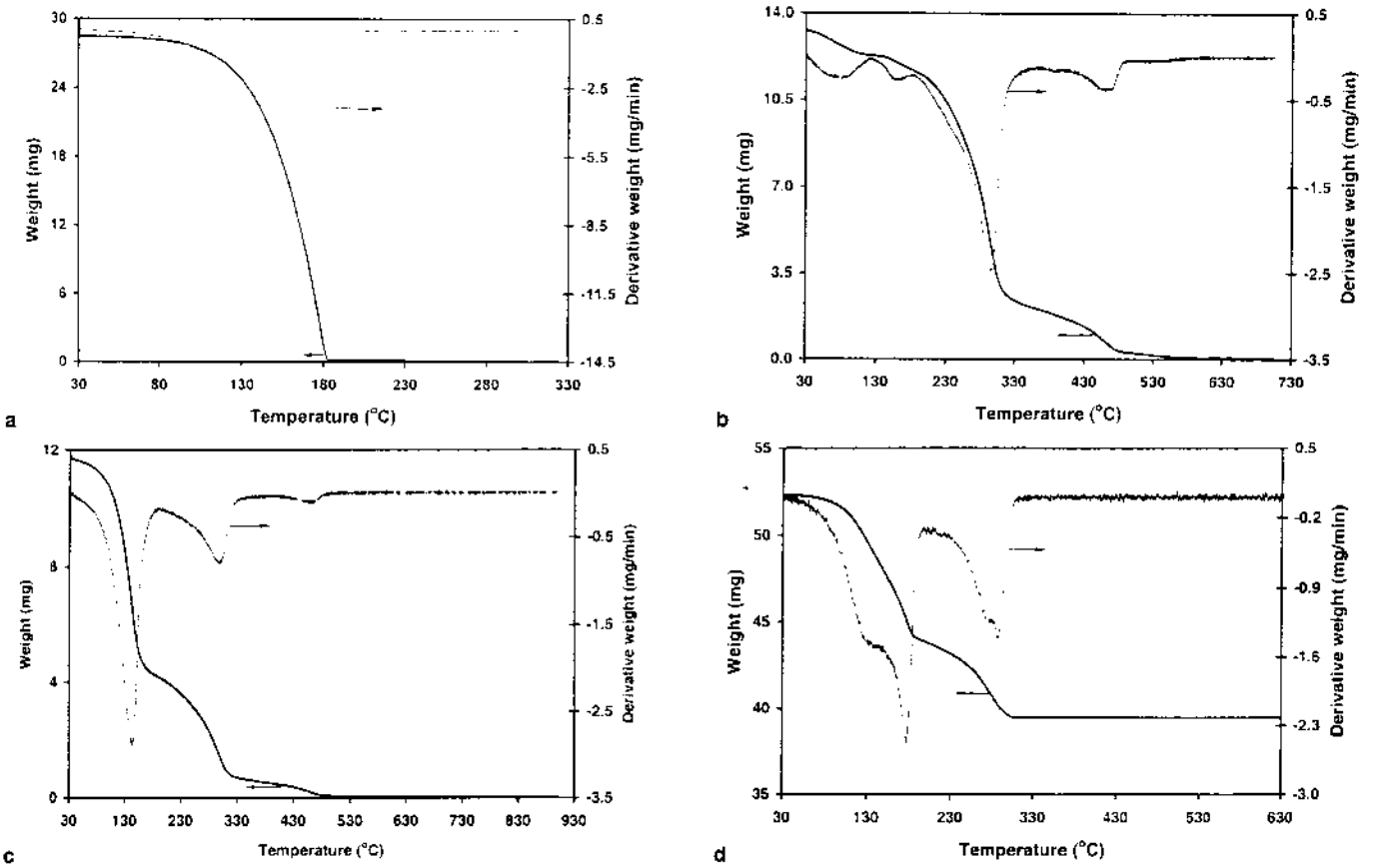

Fig. 2. Curves of weight (thick curve) and derivative weight (thin curve) versus temperature for (a) ether, (b) ethyl cellulose, (c) solution of 40 wt.% ethyl cellulose in ether, and (d) thick-film composition. The heating rate is 15°C/min.

is consistent with the three stages of weight loss in the weight versus temperature curve (Fig. 2c). Based on Refs. 2 and 34, the burnout steps from low temperature to high temperature are believed to be associated with (1) the removal of low molecular-weight components (mainly consisting of ether), (2) the thermal decomposition of ethyl cellulose, and (3) the oxidative degradation of the remaining ethyl cellulose. Compared to the third segment of the weight-loss curve in Fig. 2b, the third segment in Fig. 2c occurs at lower temperatures (above 320°C rather than above 460°C). This indicates that essentially complete burnout occurs at lower temperatures for the solution than for ethyl cellulose by itself.

Burnout of the organic vehicle in the thick-film paste (Fig. 2d) is different from that of ethyl cellulose by itself (Fig. 2b) or the solution of 40 wt.% ethyl cellulose in ether (Fig. 2c). It involves two steps, as shown by the two stages of the weight loss in the curve of weight versus temperature and by the two peaks at 30–200°C and 200–310°C in the derivative curve (Fig. 2d). In other words, the third stage in Fig. 2c is absent in Fig. 2d. The burnout of the organic vehicle in the thick-film paste (Fig. 2d) is believed to be associated with the removal of low molecular-weight components at low temperatures and thermal decomposition of high molecular-weight components at high temperatures.

Burnout Process Monitored by Calorimetry

Figure 3 shows the DSC thermograms of (a) ether, (b) ethyl cellulose, (c) a solution of 40 wt.% ethyl cellulose in ether, and (d) thick-film paste. The heating rate was 7°C/min. Evaporation of the ether resulted in an endothermic peak with an onset temperature of about 155°C (Fig. 3a), a temperature in the range from 110°C to 185°C in which significant weight loss occurs (Fig. 2a). Hence, the DSC onset temperature of 155°C is above the weight-loss onset temperature of 110°C. The difference is attributed to the lid of the DSC sample pan hindering the evolution of the gaseous components. The DSC onset temperature rather than the DSC peak temperature is used in this paper. It is reproducible to within ±5°C.

The large exothermic peak in Fig. 3b, with an onset temperature of 240°C, is mainly caused by the thermal decomposition of ethyl cellulose. Soot was visually found to remain in the pan after the DSC testing for ethyl cellulose and for the solution of ethyl cellulose in ether. A possible reason for the soot is that the limited air flow caused the organic component to be partially trapped in the pan, thus resulting in incomplete burnout. This notion is supported by TGA testing conducted with a specimen that was not covered. Indeed, no soot was visually observed after the TGA testing with the same heating rate as used in the DSC testing.

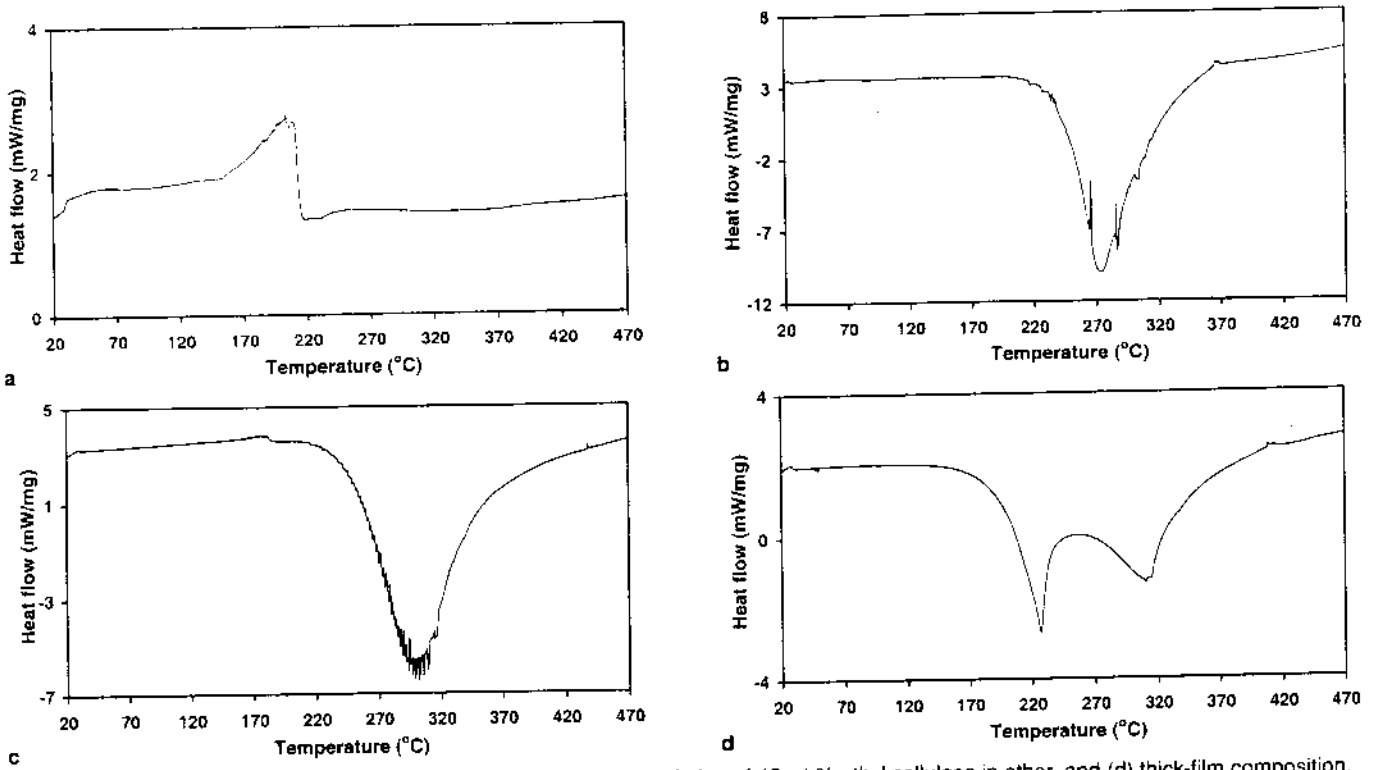

Fig. 3. The DSC thermograms of (a) ether, (b) ethyl cellulose, (c) a solution of 40 wt.% ethyl cellulose in ether, and (d) thick-film composition.

In contrast to the three-stage weight loss for ethyl cellulose by itself (curve b in Fig. 1), only one main DSC peak is present in Fig. 3b. This suggests that the DSC technique is less sensitive than the TGA technique for detecting the oxidation of the remaining ethyl cellulose and of the residue.

The DSC result for the solution of 40 wt.% ethyl cellulose in ether (Fig. 3c) shows one exothermic peak with an onset temperature of 245°C caused by thermal decomposition of ethyl cellulose. Compared with Fig. 3b, many more small exothermic peaks occur within the large exothermic-peak envelope. The difference between Fig. 3b and c means that ether affects the burnout of ethyl cellulose.

In contrast to the solution of 40 wt.% ethyl cellulose in ether (Fig. 3c), the DSC thermogram of the thick-film paste (Fig. 3d) mainly consists of two overlapping exothermic peaks. The onset temperature of the first peak is 210°C. The two overlapping peaks are probably caused by burnout of ether and the thermal decomposition of ethyl cellulose, respectively. This two-stage burnout process is consistent with the TGA curve (Fig. 1d). That the lower temperature peak in Fig. 3d is due to the burnout of ether is supported by Fig. 2a of Ref. 37, which shows only one exothermic peak corresponding to the higher temperature peak in Fig. 3d for the case in which DSC testing of the thick-film paste is conducted after drying the thick film in air for two days. In other words, the lower temperature DSC peak in Fig. 3d is present only when the thick-film paste has not undergone drying prior to DSC testing.

Drying Process

Drying of the solution of 40 wt.% ethyl cellulose in ether was not observed after exposure in air at room temperature for one month. However, drying of the ether alone in air at room temperature was observed after just a few days. This means that ethyl cellulose impedes evaporation of ether because of the interaction of ether with ethyl-cellulose molecules in the solution. This may be the reason for the many small exothermic peaks lining the large exothermic peak in Fig. 3c. In contrast to the drying of the solution of ethyl cellulose in ether, drying of the thick-film paste was observed after exposure in air at room temperature for just about 2 days. This means that the metal particles in the paste facilitate the evaporation of ether probably because of diminished interaction among the organic molecules. In a similar vein, the metal particles may facilitate the burnout of ether, thus resulting in the lower-temperature exothermic peak in Fig. 3d.

Effect of Heating Rate on the Burnout Process

Figure 4 shows the typical TGA curves of ethyl cellulose at heating rates of (a) 7°C/min, (b) 15°C/min, and (c) 50°C/min. Only the portions of the curves above 450°C are shown. At the same temperature, the weight loss was more at a lower heating rate, as expected from kinetic consideration. The weight loss was less than 100%, even at the highest temperature of 900°C, whatever the heating rate. This is due to the residue (visually observed in the TGA sample pan) after thermal decomposition and oxidative

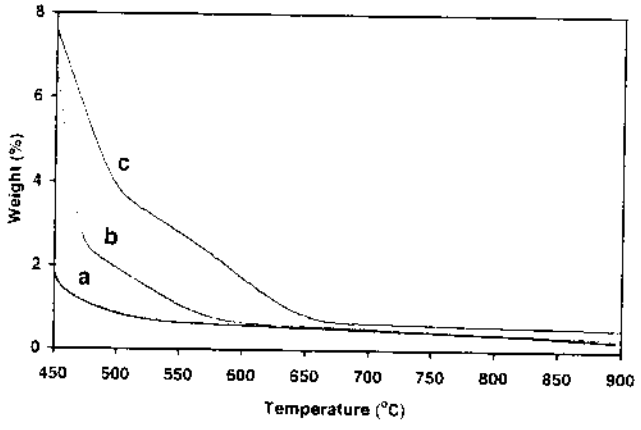

Fig. 4. Curves of weight versus temperature for ethyl cellulose at heating rates of (a) 7°C/min, (b) 15°C/min, and (c) 50°C/min.

degradation. The leveling off of the weight loss was attained at a lower temperature when the heating rate was lower.

Table II shows the remaining weight during heating of ethyl cellulose at various temperatures during TGA testing at different heating rates. Burnout of about 99% of ethyl cellulose (i.e., 1% weight remaining) occurred at 480°C, 550°C, and 650°C at heating rates of 7°C/min, 15°C/min, and 50°C/min, respectively. This dependence on the heating rate is expected, based on kinetic consideration. The weight loss was less than 100% even at a high temperature of 900°C (not shown in Table II). This is consistent with a residue, which was visually observed in the TGA sample pan when the heating rate was 50°C/min. The residue was not observed when the heating rate was 7°C/min or 15°C/min. Because of the residue, complete burnout can be assumed if the remaining weight is less than 0.5%.

Table III shows the remaining weight during heating of the solution of 40 wt.% ethyl cellulose in ether at selected temperatures during TGA testing at different heating rates. More solution can be burnt out at temperatures lower than 450°C with a heating rate of 50°C/min than 15°C/min. However, above 450°C more burnout of the solution can be realized at the lower heating rate, i.e. 15°C/min. With a heating rate of 50°C/min, about 0.65% of the solution remained at 600°C, and no more weight occurred with subsequent continuous heating up to 900°C. A residue was visually observed after TGA testing.

Figure 5 shows TGA curves of the thick-film paste at heating rates of 15°C/min (curve a), 30°C/min (curve b), and 50°C/min (curve c). Heating rates above 50°C/min were not feasible because of the limitation of the TGA system used. Each curve can be divided into two segments, without considering the leveled-off portion that occurred after the two segments. The first segment ends at 132°C, 173°C, and 190°C for heating rates of 15°C/min, 30°C/min, and 50°C/min, respectively. Complete decomposition of the remaining ethyl cellulose, as indicated by the leveling off of the TGA curve at 75% in Fig. 5, occurred at 287°C, 307°C, and 308°C for heating rates of 15°C/min, 30°C/min, and 50°C/min, respectively. Thus, a lower heating rate resulted in complete burnout at a lower temperature, as also observed in Fig. 4.

Effect of the Amount of Ethyl Cellulose in the Solution on the Burnout Process

Figure 6 and Table IV show the TGA results of the solution of 70 wt.% (curve a in Fig. 6) and 40 wt.% (curve b in Fig. 6) ethyl cellulose in ether at a heating rate of 15°C/min. Only the portions of the curves above 450°C are shown in Fig. 6. Complete burnout was delayed by having a higher concentration of ethyl cellulose. For instance, the remaining weight at 480°C is 2.4 wt.% and 0.74 wt.%, respectively, for solutions of 70 wt.% and 40 wt.% ethyl cellulose, respectively, as shown in Table IV.

A smaller amount of ethyl cellulose in the solution is helpful for obtaining complete burnout at a lower

Table II. The Remaining Weight (%) during Heating of Ethyl Cellulose at Various Temperatures during TGA Testing at Different Heating Rates

	Temperature (°C)								
Heating Rate (°C/min)	400	450	480	500	550	600	650	700	750
7	11.95	1.82	1.06	0.85	0.65	0.58	0.54	0.48	0.44
15	12.89	6.71	2.34	1.94	1.07	0.65	0.58	0.53	0.47
50	11.01	7.62	5.19	3.89	2.81	1.72	0.85	0.65	0.62

Table III. The Remaining Weight (%) during Heating of Solution of 40 wt.% Ethyl in Ether at Various Temperatures during TGA Testing at Different Heating Rates

	Temperature (°C)								
Heating Rate (°C/min)	400	450	480	500	550	600	650	700	750
15	4.07	2.22	0.74	0.59	0.48	0.44	0.43	0.42	0.38
50	3.36	1.65	0.99	0.88	0.74	0.65	0.64	0.64	0.67

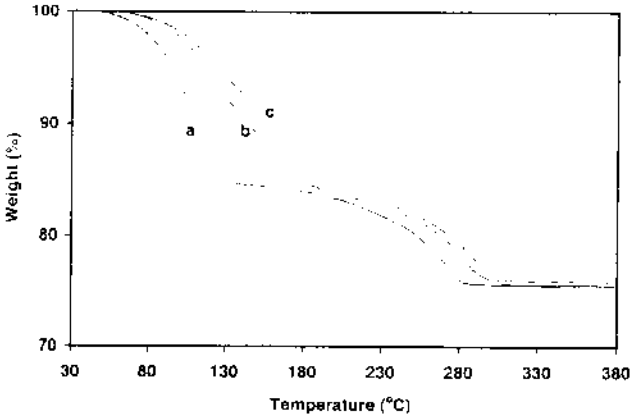

Fig. 5. Curves of weight versus temperature for thick-film paste at heating rates of (a) 15°C/min, (b) 30°C/min, and (c) 50°C/min.

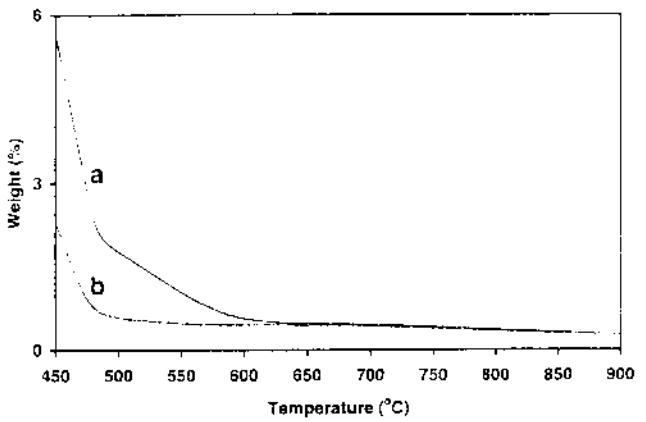

Fig. 6. Curves of weight versus temperature for solution of (a) 70 wt.% ethyl cellulose in ether and (b) 40 wt.% ethyl cellulose in ether. The heating rate is 15°C/min.

temperature. On the other hand, the ethyl cellulose must be sufficient for attaining a high viscosity, as needed for obtaining good green strength of the thick film after printing.

Effect of Interrupted Heating on the Burnout Process

Interrupted heating refers to heating to an intermediate temperature (160–385°C in this work), holding at the intermediate temperature for a certain time period (15–30 min in this work), and then heating to a high temperature (500°C or 900°C in this work). The interrupted heating was conducted for the purpose of allowing extra time for the organic burnout, which is a process that does not require high temperatures. Table V shows the remaining weight of the solution of 40 wt.% ethyl cellulose in ether after heating at 160°C for 15 min, 300°C for 30 min, or 385°C for 30 min, each followed by heating to 900°C, all at a heating rate of 15°C/min. The remaining weight is only 33.6 wt.% after heating at 160°C for 15 min. Because the original solution contained 40 wt.% ethyl cellulose, this means that complete evaporation of ether occurred at 160°C after maintaining for 15 min. Since 33.6% is less than 40%, this also means that a part of the ethyl cellulose was burnt out at 160°C. Almost complete burnout of the organic components occurred after heating at 385°C for 30 min, as shown by the remaining weight of only 1.04%. After maintaining at 300°C for 30 min, there was still about 5 wt.% residue. The amount of residue above 400°C is slightly smaller for the case of interrupted heating at 160°C for 15 min than that of interrupted heating at 300°C for 30 min, as shown in Table V. This shows that complete evaporation of the ether at low temperatures (such as 160°C) helps subsequent burnout of ethyl cellulose because of the diminished interaction between the ether and ethyl cellulose during subsequent burnout.

Figure 7 shows the DSC curves of the thick-film paste during interrupted heating from 20°C to

Table IV. The Remaining Weight (%) during Heating of A (Solution of 40 wt.% Ethyl Cellulose in Ether) and B (Solution of 70 wt.% Ethyl Cellulose in Ether) at Various Temperatures during TGA Testing at a Heating Rate of 15°C/min

	Temperature (°C)								
Heating Rate (°C/min)	**400**	**450**	**480**	**500**	**550**	**600**	**650**	**700**	**750**
A	4.07	2.22	0.74	0.59	0.48	0.44	0.43	0.42	0.38
B	9.05	5.63	2.40	1.79	1.05	0.57	0.49	0.46	0.42

Table V. The Remaining Weight (%) after Heating the Solution of 40 wt.% Ethyl Cellulose in Ether

	Temperature (°C)											
Processing	**160**	**300**	**385**	**400**	**450**	**480**	**500**	**550**	**600**	**650**	**700**	**750**
A	33.55	10.7	—	3.69	1.41	0.61	0.54	0.42	0.38	0.33	0.30	0.21
B	—	5.07	—	4.08	2.03	0.82	0.69	0.52	0.45	0.43	0.41	0.37
C	—	—	1.04	0.98	0.68	0.46	0.44	0.40	0.38	0.35	0.34	0.31

A: Maintaining at 160°C for 15 min and then heating to 900°C at a heating rate of 15°C/min.
B: Maintaining at 300°C for 30 min and then heating to 900°C at a heating rate of 15°C/min.
C: Maintaining at 385°C for 30 min and then heating to 900°C at a heating rate of 15°C/min.

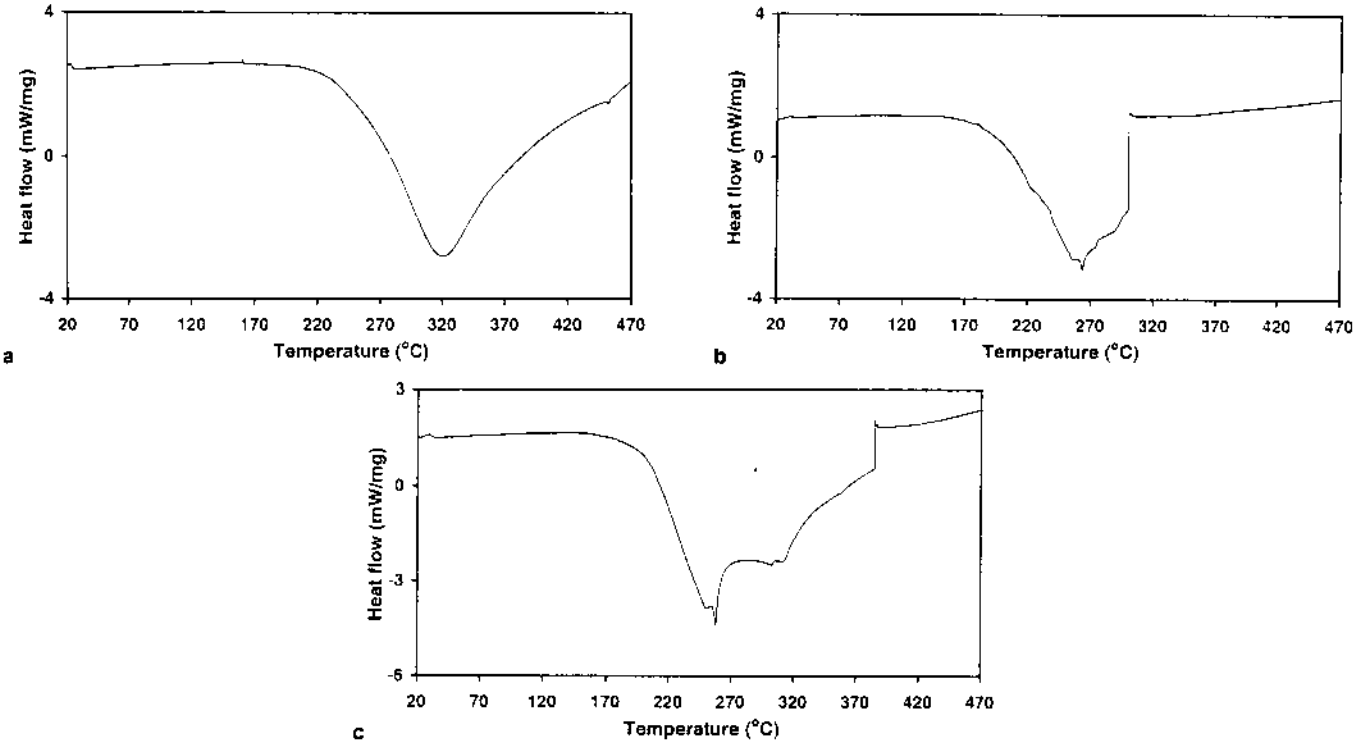

Fig. 7. The DSC thermograms of thick-film paste after heating at (a) 160°C for 30 min, (b) 300°C for 30 min, and (c) 385°C for 30 min, each followed by heating to 500°C, all at a heating rate of 15°C/min.

500°C, with interruptions at (a) 160°C for 30 min, (b) 300°C for 30 min, and (c) 385°C for 30 min. Except for (a), the isothermal portion of the interrupted heating is accompanied by isothermal heat flow, which results in a vertical line in the plot of heat flow versus temperature. According to the TGA result (Table V), 66 wt.% of the solution of 40 wt.% ethyl cellulose in ether was burnt out right after the interruption at 160°C for 15 min. However, the vertical line at 160°C in (a) is almost absent, indicating that burnout of the low molecular-weight components caused negligible heat flow. So TGA appears to be a more sensitive method than DSC for the investigation of the organic burnout. However, DSC can distinguish between endothermic and exothermic processes, whereas TGA cannot. Figure 7a shows that there is one exothermic peak, with an onset temperature of 245°C, as caused by the thermal decomposition of ethyl cellulose. In contrast, Fig. 7b shows that the thermal decomposition of ethyl cellulose is complete immediately after the isothermal period at 300°C. Thus, isothermal holding at 300°C for 30 min helps the completion of the thermal decomposition at a relatively low temperature. Figure 7c shows two overlapping exothermic peaks with the onset temperature of the first peak around 236°C. The burnout was complete immediately after the isothermal heating at 385°C for 30 min. The first exothermic peak is probably caused by the burnout of the organic molecules with low molecular weight, including parts of the ether and ethyl cellulose. The second exothermic peak is probably due to the burnout of the molecules with high molecular weight. In Fig. 7a, only the second peak of Fig. 7c was observed because the isothermal heating at 160°C for 30 min removed the low molecular-weight component. Figure 7b shows one exothermic peak with the onset temperature of about 228°C. It corresponds to the first peak in Fig. 7c and is caused by the burnout of small organic molecules. The second peak of Fig. 7c is absent in Fig. 7b because the isothermal heating at 300°C for 30 min in Fig. 7b causes the removal of the high molecular-weight component.

Microscopy of Thick Films after Firing

Figure 8a–c, respectively, shows the typical surface morphology of the thick-film composition after firing in air at 300°C, 350°C, and 385°C for 30 min. Necking between the silver particles was observed after firing, even for a low firing temperature of 300°C. The necks are indicated by arrows in Fig. 8. More necking occurred as the firing temperature was increased because of the enhanced flow of silver. The TGA result in Table I shows that organic burnout is not complete after heating at 300°C. Thus, the burnout of the organic vehicle and the necking between silver particles are two processes that may overlap in time during heating. The overlap may hinder the burnout process as the organic component may be trapped between the necked silver particles. Increased separation of these two processes by interrupted heating helps the burnout to be more complete.

Technical Implications

For reducing the processing cost and minimizing the oxidation of metal components in a thick-film

Fig. 8. Surface morphology of the thick-film composition after firing in air at (a) 300°C, (b) 350°C, and (c) 385°C for 30 min.

paste, manufacturers of commercial thick-film pastes typically give a recommended heating rate ranging from 60°C/min to 100°C/min. The present research demonstrates that incomplete burnout of the organic vehicle may occur, particularly when the heating rate is high (e.g., 50°C/min, Table III). Even at a low heating rate, incomplete burnout occurs, though it can be alleviated by giving extra time at a low temperature (e.g., 160°C for 15 min) during firing for the organic burnout to occur.

Increase of the ethyl-cellulose content in the organic vehicle hinders burnout, so the ethyl-cellulose content should be kept low—just enough for the paste to be rhelogically acceptable.

Most commercial thick-film pastes use glass frit as the binder. For a glass-containing silver-particle (same size as those of this paper) thick-film paste, formation of extensive silver network occurs, and silver particles lose their initial morphology upon heating around 400°C[37] while the corresponding temperature for the glass-free thick-film paste of this work is about 480°C (supporting SEM photo obtained but not shown here). Thus, the overlap of the organic burnout and silver-particle necking processes occurs for glass-containing thick films as well as glass-free thick films. Thus, the findings of this paper should be useful for glass-containing thick films as well.

The silver particles facilitate both drying at room temperature and burnout upon heating. The severity of the effect of metal particles may depend on the metal composition, but the role of the metal composition has not been studied in this work.

CONCLUSIONS

For an organic vehicle, in the form of ethyl cellulose dissolved in ether, the organic burnout process in air involves primarily the thermal decomposition of ethyl cellulose, followed by a minor step at higher temperatures. The minor step is probably oxidative degradation.

The evaporation of ether by itself is almost complete upon heating to 185°C at a heating rate 15°C/min. The burnout of ethyl cellulose by itself is 80% complete upon heating to 320°C at a heating rate 15°C/min and 98% complete upon heating to 475°C at a heating rate 15°C/min. The presence of ether together with dissolved 40 wt.% ethyl cellulose facilitates the burnout of ethyl cellulose, so that 93% of the solution is burnt out upon heating to 320°C at a heating rate 15°C/min. The higher the ethyl-cellulose content (70 wt.% versus 40 wt.%) in the ether solution is, the higher the temperature required for complete burnout is. The higher the heating rate in the range from 15°C/min to 50°C/min is, the larger the amount of residue after burnout at the same temperature (in the range from 480°C to 750°C) is, as observed for both ethyl cellulose by itself and 40 wt.% ethyl cellulose dissolved in ether. By interrupting the heating at 160°C for 15 min, the amount of residue after subsequent burnout at a temperature up to 900°C is diminished. By interrupting the heating at either 300°C or 385°C for 30 min, the temperature required for complete burnout is reduced.

The addition of silver particles to the organic vehicle (40 wt.% ethyl cellulose in ether) facilitates both drying at room temperature and organic burnout upon heating, so that drying occurs in 2 days (rather than > 1 month) and complete burnout (rather than 80% burnout) occurs at 320°C for a heating rate 15°C/min.

Necking of the silver particles occurs after heating at temperatures as low as 300°C for 30 min. The temporal overlap of the organic burnout and silver-particle necking processes apparently interferes with the burnout process. As a result, increased separation of these two processes by interrupted heating at 160°C for 15 min prior to heating at higher temperatures helps the burnout to be more complete.

REFERENCES

1. L.A. Salam, R.D. Matthews, and H. Robertson, *J. Eur. Ceram. Soc.* 20, 1375 (2000).
2. A. Das, G. Madras, N. Dasgupta, and A.M. Umarji, *J. Eur. Ceram. Soc.* 23, 1013 (2003).
3. Z.-P. Xie, Y.-B. Cheng, and Y. Huang, *Mater. Sci. Eng.* A34[0] 20 (2003).
4. D.R. Hammond and S.H.W. Hankin, *Thermochim. Acta* 192, 65 (1991).
5. F. Dogan, J.-H. Feng, and L.G. Ferguson (U.S. patent 6,447,712, 10 September 2002).
6. P.S. Apte, E.S. Tachauer, and T.K. Solomon (World Intellectual Property Organisation patent WO9704958, 13 February 1997).

7. K.J. Voorhees, S.F. Baugh, and D.N. Stevenson, *Thermochim. Acta* 274, 187 (1996).
8. C.M. Lobley and T.X. Guo, *Mater. Sci. Technol.* 14, 1024 (1998).
9. R.M. German, *Advances in Powder Metallurgy and Particulate Materials—1996* (Princeton, NJ: Metal Powder Industries Federation, 1996), p. 10.3.
10. H.H. Angermann and O. Van Der Biest, *Mater. Manuf. Processing* 10, 439 (1995).
11. Z. Shi and Z.X. Guo, *Acta Mater.* 51, 899 (2003).
12. K.W. Kirby, A.T. Jankiewicz, R.F. Lowell, and R.L. Hallse (U.S. patent 6,083,452, 4 July 2000).
13. J.M. Vihtelic, P.D. Jackson, J.E. Kresta, and K.C. Frisch (European patent EP1023958, 2 August 2000).
14. T.A. Guiton and L.K. Mills (European patent EP0691944, 17 January 1996).
15. J. Wang, *J. Am. Ceram. Soc.* 75, 2627 (1992).
16. Z. Shi, Z.X. Guo, and J.H. Song, *Acta Mater.* 50, 1937 (2002).
17. Z. Shi, Z.X. Guo, and J.H. Song, *Mater. Sci. Technol.* 16, 843 (2000).
18. J. Fan, B. Huang, X. Qu, and Y. Li, *Trans. Nonferrous Met. Soc. China* 9, 93 (1999).
19. D. Rodrigues and A.P. Tschiptschin, *Mater. Sci. Forum* 299–300, 439 (1999).
20. M. Zhu and D.D.L. Chung, *J. Electron. Mater.* 23, 541 (1994).
21. Z. Liu and D.D.L. Chung, *J. Electron. Packaging* 123, 64 (2001).
22. Z. Liu and D.D.L. Chung, *J. Electron. Mater.* 30, 1458 (2001).
23. L.A. Xue and J. Piascik (U.S. patent 6,306,208, 23 October 2001).
24. L.A. Xue and J. Piascik (U.S. patent 6,248,680, 19 June 2001).
25. J. Qiu, J. Tani, Y. Kobayashi, T.Y. Um, and H. Takahashi, *Smart Mater. Struct.* 12, 331 (2003).
26. S.A. Kanber, A.H. Ibraheim, and L.A. Jamil, *Thermochim. Acta* 177, 329 (1991).
27. A. Dwivedi and R.F. Speyer, *Thermochim. Acta* 247, 431 (1994).
28. H. Hoppert, *Thermochim. Acta* 20, 81 (1977).
29. P. Sung, K. Gary, D. Leon, and T. Song, *Solid Freeform Fabrication Symp. Proc.* (Austin, TX: University of Texas at Austin, 1998), p. 671–672.
30. A. Maximenko and O. Van Der Biest, *J. Eur. Ceram. Soc.* 18, 1001 (1998).
31. J. Jarrige, J.P. Lecompte, J. Mullot, and G. Muller, *J. Eur. Ceram. Soc.* 17, 1891 (1997).
32. M. Trunec and J. Cihlar, *J. Eur. Ceram. Soc.* 17, 203 (1997).
33. Y. Zeng, D. Jiang, and P. Greil, *J. Eur. Ceram. Soc.* 20, 1691 (2000).
34. L.A. Salam, R.D. Matthews, and H. Robertson, *J. Eur. Ceram. Soc.* 20, 335 (2000).
35. M. Trunec and J. Cihlar, *J. Eur. Ceram. Soc.* 22, 2231 (2002).
36. J.I. Eldridge, D.R. Wheeler, R.R. Bowman, and A. Korenyi-Both, *J. Mater. Res.* 12, 2191 (1997).
37. Z. Liu and D.D.L. Chung, *J. Electron. Mater.* 33, 194 (2004).